J MATER SCI **41** (2006) 4239–4245

Nanoparticle-induced enhancement in fracture toughness of highly loaded epoxy composites over a wide temperature range

J. T. HAN, K. CHO*
Department of Chemical Engineering, Pohang University of Science and Technology, Pohang, 790-784, Korea
E-mail: kwcho@postech.ac.kr

The fracture toughness of an epoxy molding compound (EMC) has been enhanced over a wide temperature range by the addition of a very low volume fraction of silica nanoparticles to the EMC filled with micro-silica particles, which induces macroscopic crack deflection and plastic deformation in front of the crack tip. To evaluate the fracture toughness (G_{IC}) of these materials, the single edge notched bending (SENB) test was performed for a wide range of temperatures (from ambient temperature to 230°C). The fracture toughness of the nano-silica filled EMCs was found to be improved in this temperature range by as much as a factor of two. Investigation of the fracture surfaces revealed that the micro-silica particles are covered with deformed matrix materials, which implies that the silica nanoparticles induced the crack to move into the interface between the micro-silica particles. Fractography results suggest that the silica nanoparticles act as surface modifiers of the micro-silica particles, which results in crack deflection and plastic deformation.

1. Introduction

As well as enabling property modification, the incorporation of fillers in thermosets can result in cost reduction, since most such fillers are of low cost relative to polymers. Fillers can be used to modify the properties of the cured polymer in a wide variety of ways. Some examples of properties readily modified by the incorporation of fillers are mechanical properties such as stiffness, hardness, strength, and toughness, and thermal properties such as expansion, conductivity, and thermal decomposition [1–3]. In particular, highly filled epoxy composites, i.e. epoxy molding compounds (EMCs), have been widely used in electronic packaging. One of the key issues in the use of EMCs is the improvement of their fracture toughness at elevated temperatures. There are numerous studies of the toughening of EMCs by the addition of micron-size inorganic particles into the epoxy matrix; some mechanisms based on fracture mechanics for the resulting toughening have been suggested [4–8]. In that system, it has shown that the main crack propagation was hampered by large particles and a damage zone was formed at the main crack tip region in the large particle filled resin due to crack diversion and debonding of particle/matrix interfaces. It have also found that the fracture toughness measured from single-edge-notched flexure and double torsion tests increased by adding angular and spherical particles, while flexural and tensile strengths decreased. However, these studies did not observe significant improvements in fracture toughness over a wide temperature range, but instead focused on the effects of volume fraction, shape, size and surface modification of the particles on the toughness of the epoxy composites. In general, the toughening of polymers produced by the incorporation of micron-sized inorganic particles has been explained in terms of the bowing of the crack front. The primary crack has to pass between the particles because the rigid particles resist the propagation of the crack.

Nanotechnology is now used for the improvement of the mechanical properties of materials in many fields. Of these techniques, using nanoparticles such as clay and the nano-sized particles are of particular interests [9–16]. Substantial improvements in the mechanical properties of nanocomposite polymers such as polypropylene and poly(methyl methacrylate) as a result of the

---

*Author to whom all correspondence should be addressed.

0022-2461 © *2006 Springer Science + Business Media, Inc.*
DOI: 10.1007/s10853-006-6219-2

incorporation of SiO_2, $CaCO_3$, and Al_2O_3 nanoparticles have recently been reported [17–20]. However, in spite of these improvements in the physical and mechanical properties of nanoparticle nanocomposites, the enhancement of the toughness of polymer nanocomposites over a wide temperature range has not yet been reported.

In this paper, we report that the fracture toughness of EMCs filled with micron-sized silica particles can be dramatically improved over a wide temperature range by the incorporation of even a small amount of commercially available fumed silica nanoparticles. The mechanism of this toughening was elucidated through observation of the fractured surfaces of specimens produced in the fracture toughness tests.

2. Experimental method

2.1. Materials

A biphenyl type epoxy resin (YX-4000H (YX), Yuka Shell epoxy Co.; Equivalent weight, 193 g/eq) was used. A phenol-novolac type hardener (HF-1, Meiwa Corp.; Equivalent weight, 107 g/eq) was used, with triphenyl phosphine (TTP) as a catalyst. The chemical structures of these materials are shown in Fig. 1. These resins were selected for the formation of the "epoxy molding compound" by mixing, as shown in Table I. The micron-sized silica particles used as the main filler were of a fused spherical type, with a mean particle diameter of 30 μm. The nano-sized fumed silica particles (SN) (Aldrich) we used were 11 nm in nominal diameter with a specific surface area of 255 m^2/g. γ-glycidoxypropyl triethoxysilane and wax were used as a coupling agent and releasing agent respectively.

2.2. Preparation of nanocomposites

The SN-filled EMC (SN-EMC) nanocomposites were prepared by using a two-roll mill. Firstly, the epoxy resin was premixed with silica nanoparticles. According to the recipe shown in Table I, a silica-filled master batch was mixed at the roll surface temperature of about 90°C for a proper dispersion time of 10 min to lower the degree of curing. The melt-mixed EMC was then cooled and crushed into the powder. The EMC was molded at 175°C for 5 min using a compression molder, and then fully cured at 175°C for four hours in the convection oven. SN-filled epoxy (SN-epoxy) nanocomposites without micro-silica particles were also prepared for the fracture toughness tests.

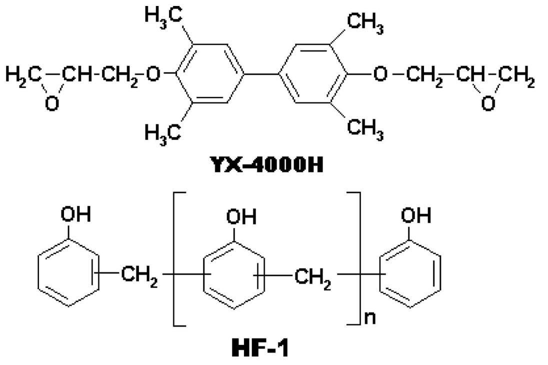

Figure 1 Chemical structure of base materials; (a) epoxy resin: YX-4000H (b) hardener: HF-1.

TABLE I Formulation of NS-EMC nanocomposite

Raw material	Parts by weight	Remark
Epoxy resin	100	Equiv. wt of epoxy 193
Hardener	41–55	Equiv. wt of phenol 107
Catalyst (TPP)	1.6–2.3	Equiv. wt ratio of epoxy/phenol = 1.0
Filler (fused silica)	80	Mean diameter = 30 μm
Nano-silica	3–5	Mean diameter = 11 nm
Coupling agent	2.9–3.1	
Releasing agent	2.1–2.4	

2.3. Characterization and property measurements

The viscoelastic properties of the SN-EMC nanocomposites such as the storage modulus, E', and the loss factor, tan δ, were determined with a DMA analyzer (TA Instrument, DMA2980). The frequency was 1 Hz and the heating rate was 3°C/min. The measurements were performed using a single cantilever device with a 17.5 mm span. The specimen dimensions were $35 \times 12.8 \times 2\ mm^3$. E' and tan δ were measured from room temperature up to temperatures beyond the rubbery state.

The critical stress intensity factor (K_{IC}) was measured using single-edge notched 3-point bending (SENB) geometry and SEN specimens of $5 \times 12 \times 60\ mm^3$, which meets the plane strain condition test according to ASTM E-399 [4]. The bending rig was placed in an oven capable of providing a temperature environment up to 230°C. The load-time curve was measured with a displacement rate of 1.3 mm/min. These tests were performed on each of the six EMC specimens.

Critical stress intensity factors were calculated from equation 1,

$$K_{IC} = \frac{3P_cS}{2BW^2}\sqrt{a}\,f(x) \tag{1}$$

where P_c is the load at fracture, a is the crack length, W is the specimen width, B is the specimen thickness, S is the span length and $f(x)$ is a geometric factor given by

$$f(x) = 1.93 - 3.07x + 14.53x^2 - 25.11x^3 + 25.8x^4$$

where, $x = a/W$.

Critical strain energy release rates (G_{IC}) were calculated from the stress intensity values using the following

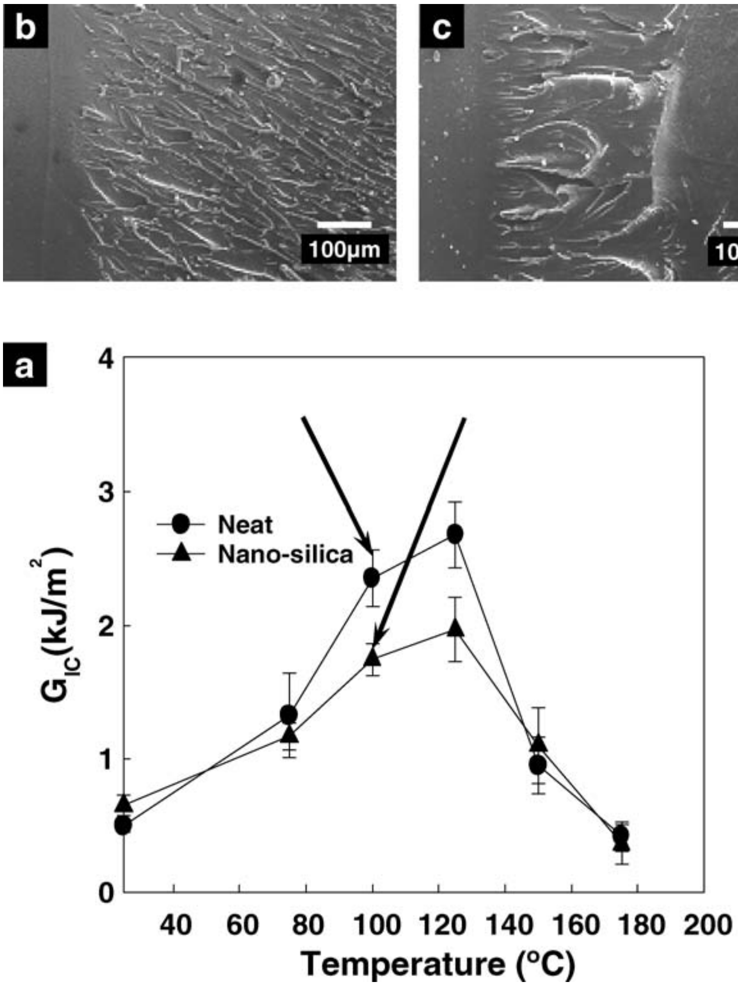

Figure 2 (a) Fracture toughness (G_{IC}) of neat epoxy resin and SN-epoxy nanocomposites without micro-silica particles as a function of temperature. Fractographies of neat epoxy resin (b) and SN-epoxy nanocomposites (c) after SENB fracture test at 75°C.

relationship:

$$G_{\mathrm{IC}} = \frac{(1-v^2)K_{\mathrm{IC}}^2}{E}$$

where v is Poission's ratio, and E is Young's modulus.

To determine the mechanism of the improvement in fracture toughness, scanning electron microscopy was performed on the fracture surfaces of the SENB specimens coated with a thin layer of platinum using a Hitachi S-4200 SEM. The accelerating voltage was 8 keV.

3. Results and discussion

Firstly, the fracture toughness of the SN-epoxy nanocomposite without micro-silica particles was determined over a wide temperature range in order to compare this with the fracture toughness of the SN-EMC nanocomposite. Fig. 2a shows the variations of the G_{IC} values of the neat epoxy resin and the SN-epoxy nanocomposite with temperature. The fracture toughness of the SN-epoxy at room temperature (RT) was found to be slightly increased by the incorporation of silica nanoparticles. Moreover, the fracture toughness of both the neat epoxy resin and the SN-epoxy nanocomposite was found to increase up to a certain temperature, followed by a drastic decrease in toughness at high temperatures, which occurs because at these temperatures the epoxy resin softens. The increase in toughness of epoxy resin at high temperature below T_g can be attributed to an increased molecular mobility of network chains resulting in the yielding of epoxy resin. However, when silica nanoparticles having hydroxyl group are incorporated in epoxy resin, the fracture toughness of nanocomposites with temperature may be lower than the neat epoxy resin because the yielding of epoxy resin can be restricted with nanosilica particles having hydroxyl group interacting with epoxy resin. Fig. 2b and c show fractographies of the SENB specimens of the neat epoxy resin and the SN-epoxy nanocomposite without micro-silica particles respectively. The SN-epoxy nanocomposite has a deformed surface in the slow crack propagation region. This result suggests that the silica nanoparticles do not restrict the macroscopic plastic deformation of the epoxy resin at temperatures above RT, because the nano-scale size (11 nm) of the filled silica nanoparticles means that the yielding of the epoxy

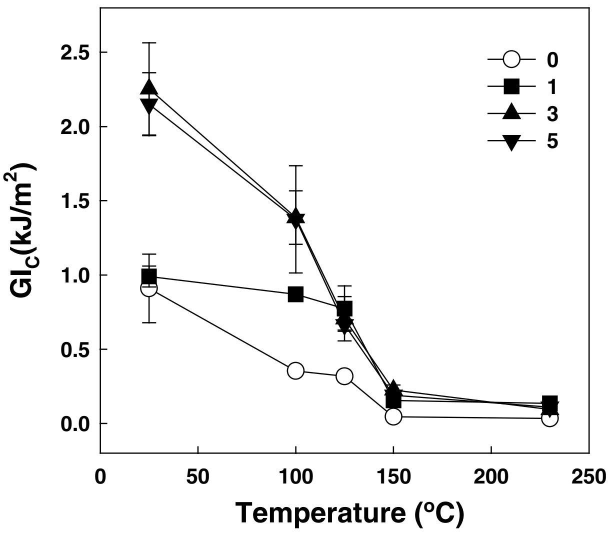

Figure 3 Fracture toughness (G_{IC}) of pristine EMC and SN-EMC nanocomposites as a function of temperature. (Values indicate the content of nanoparticles, wt.%) (●: prisitne, (■): 1 wt.%, (▲): 3 wt.%, (▼): 5 wt.%).

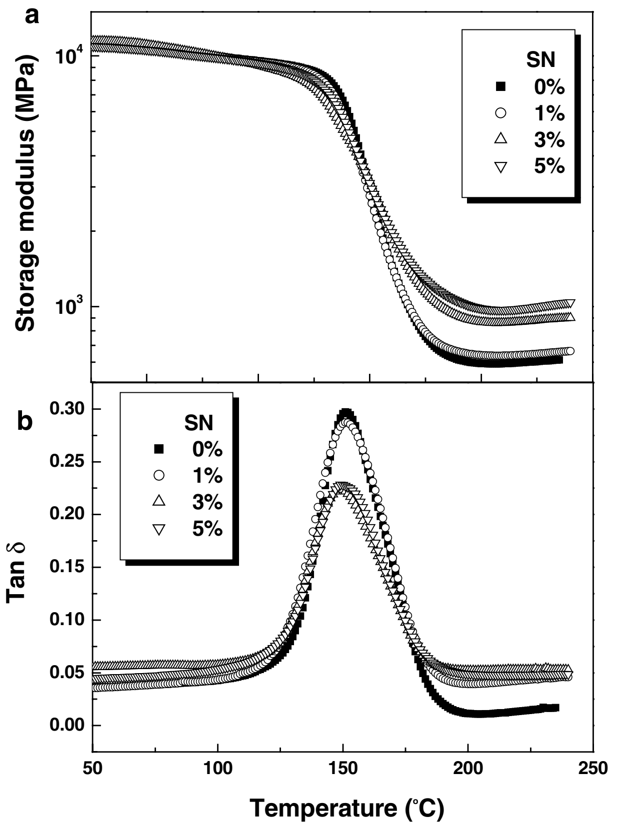

Figure 4 (a) Storage modulus and (b) tan δ of SN-EMC nanocomposite as a function of a SN content.

network in front of the crack tip is not significantly limited. The fracture toughness is dependent on the deformation behavior, in particular the yielding of the network in front of the crack tip.

Fig. 3 shows the G_{IC} values of pristine EMC and SN-EMC nanocomposites containing 80 wt.% micro-silica particles. Koh *et al.* [21] reported that the G_{IC} values of micro-sized silica-filled epoxy resins are largest at ambient temperatures and tend to decrease above and below ambient temperatures. The trend observed in this study for the variation of the G_{IC} of pristine EMC with temperature is in agreement with these results. The decrease in fracture toughness at temperatures above RT may be related to the detrimental effects of the softening of the matrix material. It has previously been demonstrated that the strength and stiffness of these materials are reduced significantly above ambient temperatures. Therefore, the beneficial effects of the toughening mechanisms that may be operative at high temperatures are outweighed by the loss of strength and stiffness, which results in a substantial reduction in their fracture toughness.

However, the G_{IC} values of the EMCs filled with a small amount of silica nanoparticles (3 to 5 wt.%) were found to dramatically increase by as much as a factor of two even at RT, as shown in Fig. 3; at RT, G_{IC} is approx. 1.0 kJ/m^2 for the pristine EMC, and approx. 2.2 kJ/m^2 for the nanocomposite EMC with 3 wt% silica nanoparticles. These results demonstrate the important role of silica nanoparticles in the toughening of highly loaded composite systems, such as EMCs filled with over 80 wt% micro-silica particles; note the contrast with epoxy nanocomposites containing no micro-silica particles. It is also remarkable that the incorporation of only a small amount of silica nanoparticles (1 wt%) was found to enhance the toughness of the EMC (300% increase) even at temperatures above 200°C; at 220°C, G_{IC} is approx. 0.013 kJ/m^2 for the pristine EMC, and approx. 0.04 kJ/m^2 for the nanocomposite EMC with 3 wt% silica nanoparticles.

Furthermore, the relationship between the dynamic mechanical properties of the EMC nanocomposites and the fracture toughness must be considered. As shown in Fig. 4, the storage modulus for the rubbery plateau region increases remarkably as a result of the addition of the silica nanoparticles, but the glass transition temperature ($T_g \sim 151°$C) is unchanged or only slightly shifted. The change in the storage modulus above T_g may affect the fracture toughness of the SN-EMC nanocomposites. However, these changes in the viscoelastic properties are not likely to be closely correlated with the fracture behavior of the EMCs, because although the E' of the 1% SN-filled EMC nanocomposite was not found to increase, its G_{IC} was found to increase by more than a factor of three.

The mechanism of the toughening of the nanocomposite EMCs was investigated by using SEM examination of the fracture surfaces of the SENB specimens. Typical fracture surfaces of pristine EMC and the SN-EMC nanocomposites at RT are shown in Fig. 5a and b respectively. The fractographies show the drastic change in the locus of failure with the addition of the silica nanoparticles. In the pristine EMC, clear particles, particle debonded regions and characteristic step structures behind particles, known as characteristic tails, were observed at RT, and the crack

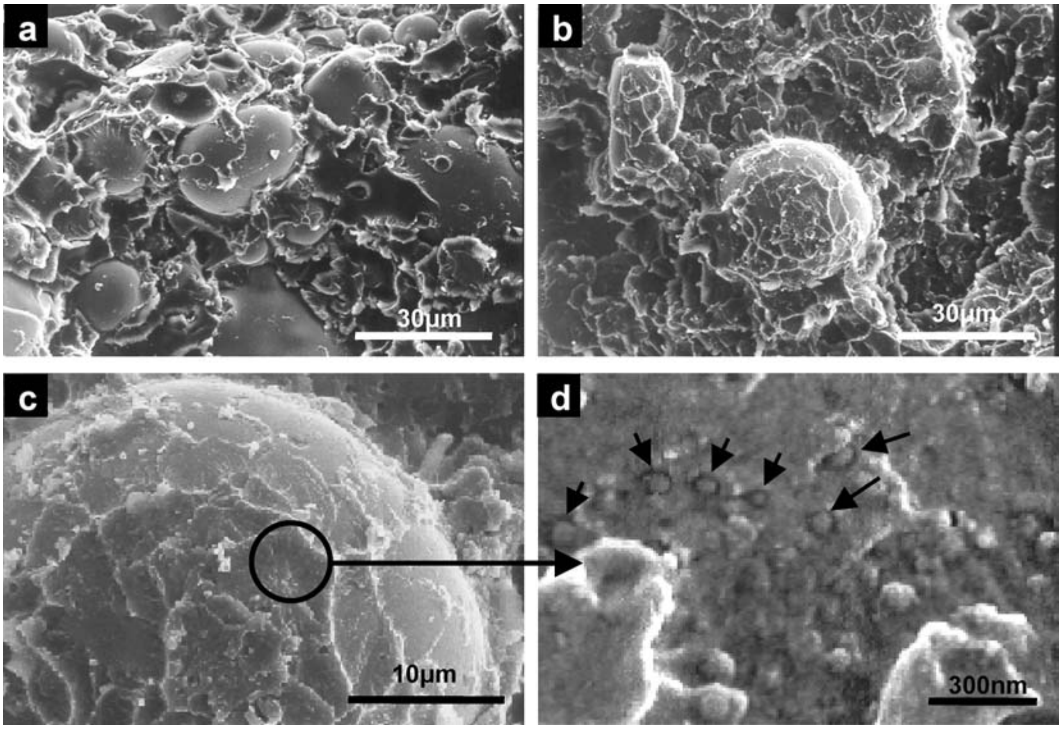

Figure 5 SEM micrographs of the fracture surfaces of the SN-EMC nanocomposite SENB test specimens at room temperature: (a) with no silica nanoparticles; (b) filled with 3% silica nanoparticles; (c) magnified image of (a); (d) magnified image of the circled region in (c), in which the arrows indicate the debonding region near the silica nanoparticles.

seems to have propagated around the particle surface (Fig. 5a). Similar results have been reported elsewhere [22–25], which were explained in terms of crack front bowing and crack tip blunting. Therefore, the fracture toughness of an EMC is higher than that of a neat epoxy resin. However, at temperatures above RT, a high loading of micro-silica particles in the epoxy resin (over 80%) results in a dramatic decrease in the fracture toughness because of the low deformation volume of the matrix materials.

In the SN-EMC nanocomposites, the micro-silica particles are mostly covered with the epoxy resin containing the silica nanoparticles, and the crack propagates through the interface between the micro-silica particles with a plastic deformation of the matrix material (Fig. 5c). This result provides evidence that the crack is deflected into the interface between the micro-silica particles and that the epoxy resin is deformed. Therefore, the improvement in the toughness at RT can be explained by crack deflection and the plastic deformation of the matrix material, which results in an increase in the crack propagation path and in the energy-dissipating events in the region immediately ahead of the crack tip. Fig. 5d shows a highly magnified image of the area circled in Fig. 5c. The arrows in Fig. 5d indicate the particle debonded region around the silica nanoparticles, which may induce crack deflection (drawn schematically in Fig. 7b) and the plastic deformation of the matrix material (drawn schematically in Fig. 7c). The fractographies of the SN-EMC nanocomposites at temperatures above the T_g

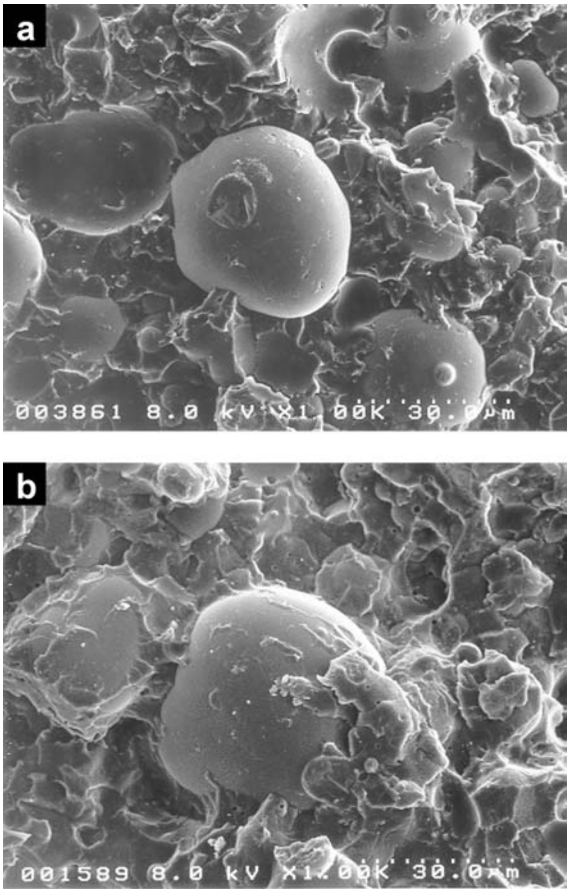

Figure 6 SEM micrographs of the fracture surfaces of SENB test specimens for (a) a pristine EMC and (b) a SN-EMC nanocomposite at 230°C.

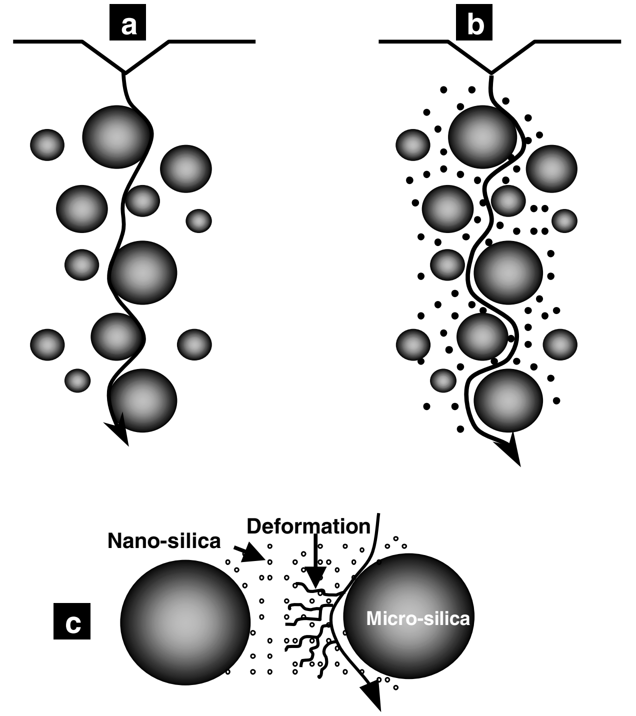

Figure 7 A schematic diagram of the crack propagation and toughening mechanism of SN-EMC nanocomposites: (a) pristine EMC, and (b) SN-EMC nanocomposites. (c) Schematic view of the deflection and plastic deformation of a matrix material induced by the silica nanoparticles.

of the epoxy resin are shown in Fig. 6. The locus of failure in the pristine EMC moves further down to the equators of the micro-silica particles due to the softening of the matrix material at temperatures above the T_g of the epoxy resin, whereas with the addition of the silica nanoparticles it moves towards the poles of the micro-silica particles.

Recently, Ash *et al.* [20] reported that the presence of alumina nanoparticles caused a decrease in the glass transition temperature of poly(methyl methacrylate), which results in a brittle-to-ductile transition in uniaxial tension with an increase in the strain-to-failure. Further, the brittle-to-ductile transition was found to depend on poor interfacial adhesion between the polymer and the nanoparticles. However, in our system the fumed silica nanoparticles containing hydroxyl groups are compatible with the matrix material, which results in good interfacial adhesion between the matrix and the nanoparticles. Therefore, we speculate that the silica nanoparticles used in our study act as surface modifiers of the micro-silica particles, which results in the significant plastic deformation of the matrix materials and in crack deflection in front of the crack tip. This mechanism can be regarded as the major contributing factor to the observed improvement in toughness over a wide temperature range.

4. Conclusion

The toughness of an epoxy molding compound was found to be dramatically improved over a wide temperature range by the incorporation of fumed silica nanoparticles. At RT as well as above the T_g of the epoxy resin, the toughness of the SN-EMC nanocomposite was found to improve by as much as a factor of two. The fractured surfaces of the nanocomposite EMC SENB test specimens were found to consist of particles covered with matrix materials, which indicates that the nanoparticles led the crack towards the interface between the micro-sized silica particles, i.e., acting as a surface modifier of the micro-silica particles, which caused the plastic deformation of the matrix material in front of the crack tip. Fractographies of the fractured surfaces revealed that crack deflection and plastic deformation are the principal factors contributing to the observed toughening at high temperatures.

Acknowledgment

This work was supported by a grant (code #: 05K1501-01010) from 'Center for Nanostructured Materials Technology' under '21st Century Frontier R&D Programs' and National Research Laboratory Program of the Ministry of Science and Technology, and BK21 program of Ministry of Education & Human Resources Development, Korea.

References

1. C. A. MAY and T. TANAKA (Ed)., "*Epoxy Resins – Chemistry and Technology*" (Marcel Dekker Inc., New York, 1973).
2. H. LEE and K. NEVILLE, "*Handbook of Epoxy Resins*" (McGrawHill, New York, 1967).
3. B. ELLIS (Ed)., "*Chemistry and Technology of Epoxy Resnis*" (Blackie & Professional, New York, 1993).
4. Y. NAKAMURA, M. YAMAGUCHI, A. KITAYAMA, M. OKUBO and T. MATSUMOTO, *Polymer* **32** (1991) 2221.
5. Y. NAKAMURA, M. YAMAGUCHI, M. OKUBO and T. MATSUMOTO, *ibid.* **22** (1992) 3415.
6. *Idem., J. Appl. Polym. Sci.* **45** (1992) 1281.
7. *Idem., ibid.* **44** (1992) 151.
8. Y. NAKAMURA, M. YAMAGUCHI, A. TANAKA and M. OKUBO, *Polymer* **34** (1993) 3220.
9. C. ZILG, R. MÜLHAUPT and J. FINTER, *Macromol. Chem. Phys.* **200** (1999) 661.
10. Z. S. PETROVIC, I. JAVNI, A. WADDON and G. BANHEGYI, *J. Appli. Polym. Sci.* **76** (2000) 133.
11. C. WANG, Y. ZHANG, L. DONG, L. FU, Y. BAI, T. LI, J. XU and Y. WEI, *Chem. Mater.* **12** (2000) 3662.
12. S. KANG, S. I. HONG, C. R. CHOE, M. PARK, S. RIM and J. KIM, *Polymer* **42** (2001) 879.
13. R. W. SIEGEL, S. K. CHANG, B. J. ASH, J. STON, P. M. AJAYAN, R. W. DOREMUS and L. S. SCHADLER, *Scripta Mater.* **44** (2001) 2062.
14. E. PETROVICOVA, R. KNIGHT, L. S. SCHADLER and T. E. TWARDOWSKI, *J. Appl. Polym. Sci.* **77** (2000) 1684.
15. *Idem., ibid.* **78** (2000) 2272.
16. E. REYNAUD, T. JOUEN, C. GAUTHIER, G. VIGIER and J. VARLET, *Polymer* **42** (2001) 8759.
17. M. Z. RONG, M. Q. ZHANG, Y. X. ZHENG, H. M. ZENG, R. WALTER and K. FRIEDRICH, *ibid.* **42** (2000) 167.
18. M. Z. RONG, M. Q. ZHANG, Y. X. ZHENG, H. M. ZENG and K. FRIEDRICH, *ibid.* **42** (2000) 3301.

19. C. M. CHAN, J. WU, J. X. LI and Y. K. CHEUNG, *Polymer* **43** (2002) 2981.
20. B. J. ASH, R. W. SIEGEL and L. S. SCHADLER, *Macromolecules* **37** (2004) 1358.
21. S. W. KOH, J. K. KIM and Y. W. MAI, *Polymer* **34** (1993) 3446.
22. J. SPANOUDAKIS and R. J. YOUNG, *J. Mater. Sci.* **19** (1984) 473.
23. J. SPANOUDAKIS and R. J. YOUNG, *ibid.* **19** (1984) 487.
24. F. F. LANGE and K. C. RADFORD, *ibid.* **6** (1971) 1197.
25. D. J. GREEN, P. S. NICHOLSON and J. D. EMBURY, *ibid.* **12** (1977) 987.

Received 10 May
and accepted 10 August 2005